The Galactic potential effects on the Solar System's minor bodies

Author: Pau Roca Acarin, procaaca27@alumnes.ub.edu
Facultat de Física, Universitat de Barcelona, Diagonal 645, 08028 Barcelona, Spain.

Advisor: Mercè Romero, mromero@fqa.ub.edu
(Dated: January 16, 2026)

Abstract: This project studies the influence of the Milky Way's galactic gravitational potential on the orbital evolution of distant Solar System minor objects. Using orbital data from Gaia Data Release 3, minor body motion is modeled through the Circular Restricted Three-Body Problem (Sun–Jupiter–minor body), with Galactic perturbations included as an external force. Two Galactic models are considered: the axisymmetric MWPotential2014 and a non-axisymmetric Spiral Arms plus MWPotential2014, both implemented with the `galpy` library. Numerical integrations are used to analyze secular variations of orbital elements over long timescales. The study focuses on the dwarf planet Eris and a hypothetical Sun-bound asteroid with a semi-major axis of 530 AU. Although galactic forces are much weaker than Solar System forces near the Sun, they produce measurable effects at large heliocentric distances: spiral arm effects are negligible near 100 AU, while both galactic components significantly influence orbital stability beyond 500 AU, with the spiral arm pitch angle playing a key role.
Keywords: Galactic potential, Minor objects orbital dynamics, Spiral Arms potential, Milky Way gravitational field, Secular perturbations, Numerical orbit integration
SDGs: Education of Quality, Terrestrial life and Industry, Innovation & Infrastructure.

I. INTRODUCTION

Over the last decade, the study of asteroids and other minor bodies has intensified significantly, driven by major advances in observational capabilities and the availability of high-precision astrometric datasets. Particularly, the *Gaia* mission has revolutionized Solar System science by providing unprecedented positional and kinematic measurements for a vast number of minor bodies, culminating in the extensive catalog inside Gaia Data Release 3 [1].

The Oort Cloud, which can extend up to 200.000 AU, contains most of the minor bodies. At such distances, the effect of the Galactic environment becomes non-negligible. Furthermore, current models of the Galactic tides date back to pre-Gaia data, with Heisler and Tremaine (1986) [2]. As such, it becomes apparent that the models need to be updated.

This work combines Gaia observations with numerical orbit integration techniques to quantify the influence of the Milky Way's Galactic gravitational potential on distant Solar System objects. Galactic tides and large-scale gravitational perturbations, while often neglected in studies of inner Solar System dynamics, are expected to play a non-negligible role in shaping the long-term orbital evolution of trans-Neptunian objects and detached bodies. The motivation of this study is to provide a first-order assessment of the contribution of the Galactic gravitational potential to minor bodies orbits. By leveraging Gaia DR3 astrometry and a simplified Galactic potential model, this work aims to establish an initial framework for understanding the role of Galactic perturbations in the long-term dynamics of distant Solar System objects.

The project is organized as follows. The **Data and Tools** section describes the observational datasets and numerical methods employed. The **Theoretical Basis** introduces the physical and mathematical framework underlying the orbital integrations and Galactic potential model. The results are then presented for the dwarf planet **Eris** and for an **example asteroid**, followed by the main **conclusions** and perspectives for future work.

II. DATA AND TOOLS

The data used for this project was extracted from the Performance verification in the Gaia Data Release 3 (GDR3), which provides orbital solutions for over 150 000 Solar System objects, following the method described in [1], section 3.5.

Since the force from the Circular Restricted Three-Body Problem (CRTBP) is expected to be orders of magnitude larger, in order to properly study the Galactic potentials, only the Solar System objects with semi-major axis greater than 40 AU are considered (see Figure 1). Numerical integrations were performed using Python-

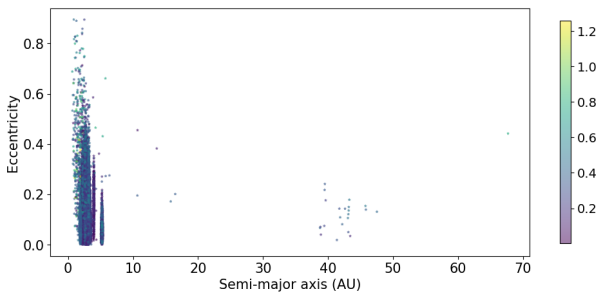

FIG. 1: Representation of the Semi-major axis of the orbit in correspondence to the eccentricity of the orbit for all asteroids in the GDR3, with a colorbar for the inclination in radians.

based tools. The equations of motion were integrated using `SciPy`'s `solve_ivp` routine, while Galactic gravitational potentials were implemented through the `galpy` library[3]. Additionally, other routines were coded as to transform between orbital elements and Cartesian coordinates, inspired by Chapter 3 of Prussing and Conway [4]. Moreover, functions to manage data, storage and analysis compatible with the GDR3 were developed.

III. THEORETICAL BASIS

Mean orbital elements are averaged Keplerian parameters that describe the long-term size, shape, and orientation of an orbit by removing short-period perturbations. They include the semi-major axis a (orbit size), eccentricity e (orbit shape), and inclination i (tilt with respect to the reference plane). The orientation is defined by the right ascension of the ascending node Ω and the argument of pericenter ω, while the mean anomaly f specifies the average position along the orbit. An image representing the orbital elements has been added in Appendix A. Thus, having the orbital elements is equivalent to having the orbit of a given object.

A. Solar System

The minor body motion is modeled using the Circular Restricted Three-Body Problem (CRTBP) for the Sun–Jupiter system, following standard formulations from Szebehely [5] and Gómez, Jorba, Masdemont and Simó [6]. The CRTBP provides a first-order approximation to Solar System dynamics dominated by the Sun–Jupiter pair. While it neglects additional planets, its simplicity allows us to isolate and compare the relative magnitude of Galactic perturbations.

The CRTBP is explained in more detail, along with the equations of motion, in Appendix B.

B. Galactic Potential

MWPotential2014: The Galactic potential, Φ_{gal}, represents the smooth and axisymmetric gravitational field of a given galaxy. The Milky Way potential (hereafter, MWPotential2014) was developed to produce a simple yet accurate model of our Galaxy (Bovy et al [7]). It consists of three distinguished parts: a Miyamoto-Nagai disk, representing disk matter of gas and stars, a Navarro-Frenk-White (NFW) model for the dark matter, and a spherical bulge potential that is exponentially cut-off at a certain radius, as explained in section 3.5 of Bovy et al (2015) [7]. A further explanation, along with its equations, is in Appendix C.

This potential is well known and incorporated into the *Galpy* library. Tests were also performed using the McMillan17, and the results are equivalent.

Spiral Arms: To incorporate a non-axisymmetric potential into the axisymmetric MWPotential2014 model, a Spiral Arms potential was created using *Galpy*. The Spiral Arms model is inspired by the one described in Eq. (8) of the Cox and Gómez [8] paper. In this project, we vary parameters such as the amplitude (amp=0.4) and the pitch angle ($\alpha = 9.5°$), while maintaining the same structure as seen in Eq. 1. The locus of the potential developed, following the aforementioned formula, is shown in Figure 2.

$$\Phi(r,\phi,z) = -4\pi G H \rho_0 \exp\left(\frac{r-r_0}{R_s}\right) \times \sum_n \left(\frac{C_n}{K_n D_n}\right) \cos(n\gamma) \left[\operatorname{sech}\left(\frac{K_n z}{\beta_n}\right)\right]^{\beta_n} \quad (1)$$

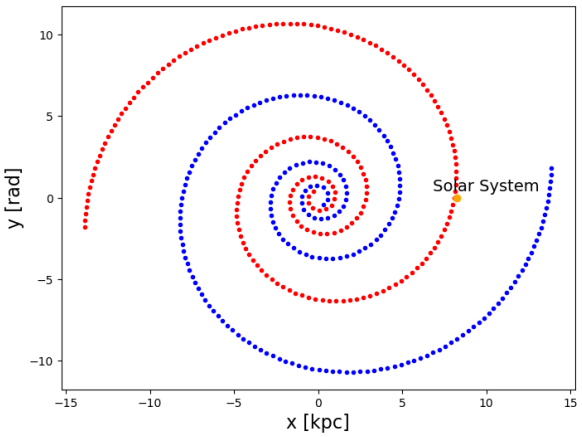

FIG. 2: Representation of the Spiral Arm Locus in the Galactic plane,the potential exerted at the Solar System position is $\Phi = -0.00044\,[\text{AU/day}^2]$, for an amp=0.4 and $\alpha = 9.5°$

C. Force comparison

In order to better understand the contributions of the Galactic Potentials, we can study the forces that each component introduces into the equations of motion.

It is distinguishable, in Figure 3, that the contribution of the CRTBP is strong only in the position of the Solar System ($\sim$ 8.25 kpc), with a force of $F_{\text{CRTBP, SS}} \simeq 5.0355 \cdot 10^{-1}\,(\text{AU/day}^2)$. Opposed to that, both the Galactic Potential and Spiral Arms forces get bigger with the Galactocentric distance, yielding $F_{\text{MWPotential2014, SS}} \simeq -8.5987 \cdot 10^{-13}\,(\text{AU/day}^2)$ and $F_{\text{Spiral Arms, SS}} \simeq -2.6177 \cdot 10^{-13}\,(\text{AU/day}^2)$ at the position of the Solar System.

Although the Galactic force is many orders of magnitude smaller ($F_{\text{MWPotential2014}} \ll F_{\text{CRTBP}}$) at the solar position, its continuous action $\int F_{\text{MWPotential2014}} \cdot dt$ over a Myr can produce measurable secular changes in orbital elements. Because of this crucial distinction, the addition of the Galactic Potential and the Spiral Arms should be treated as a perturbation inside the equations of motion.

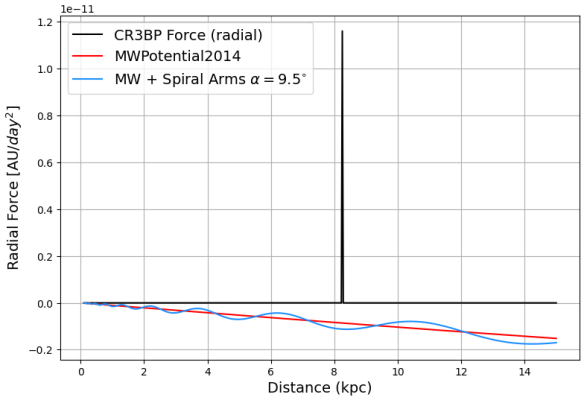

FIG. 3: Radial forces for the CRTBP and the two potentials that are going to be studied in AU/day^2. The x-axis is the distance to the Galactic center (kpc).

IV. RESULTS OF 136199: ERIS

The dwarf planet studied throughout this section is the farthest Solar System object that the GDR3 catalog offers. This dwarf planet was given the identification tag 136199, or commonly known as *Eris*, which has a distance at the aphelion of $\simeq 97.6$ AU. The GDR3 catalog includes the mean orbital elements of Eris.

$$a = 67.696\ AU \quad ; \quad e = 0.442 \quad ; \quad i = 0.770\ rad$$
$$\Omega = 0.627\ rad \quad ; \quad \omega = 3.570\ rad \quad ; \quad f = 2.638\ rad$$

The integration time will be set at $t_{integral} = 10^7$ days in 200.000 steps. This amount of time is equivalent to almost 50 Eris years, but because our force units are AU/day^2, the units of dt and $t_{integral}$ are days. The integration will yield a trace that determines the trajectory over time, and the effects by certain potentials can be extracted.

1^{st} Case (CRTBP): The trajectory evolution of Eris, governed by the CRTBP equations of motion, establishes a benchmark against which Galactic potentials can be compared. Figure 4 illustrates, in black, the integrated CRTBP trajectory, for which the final orbital elements show no variation beyond the associated error. Confirming that the CRTBP is an excellent first approximation of the Solar System potential.

2^{nd} Case (MWPotential2014): The inclusion of a Galactic potential in the equations of motion alters the orbital behavior over the course of the integration. Although the influence of the Galactic potential is several orders of magnitude smaller than that of the CRTBP, the continuous application of Galactic acceleration throughout the integration introduces a measurable perturbation to the orbit. A comparison of the two solutions is shown at the top of Figure 4, where the CRTBP solution (black) serves as a reference, and the trajectory including the MWPotential2014 (blue) exhibits a precession-like deviation in a preferred direction. This time, the changes in the orbital elements are noticeable, most notably in the semi-major axis, eccentricity, and inclination of the orbit.

$$a = 66.749\ AU \quad ; \quad e = 0.566 \quad ; \quad i = 0.665\ rad$$
$$\Omega = 0.559\ rad \quad ; \quad \omega = 3.525\ rad \quad ; \quad f = 0.965\ rad$$

3^{rd} Case (MWPotential2014 + Spiral Arms): Adding the Spiral Arms contribution (with a pitch angle of $\alpha = 9.5°$) to the MWPotential2014 results in a more accurate depiction of the Galactic potential. The results can be seen in the bottom panel of Figure 4. There is an obvious similarity to the results obtained in the **2^{nd} Case**, where only the MWPotential2014 was taken into account. The mean orbital elements are almost identical, which shows that the addition of a Spiral Arms potential to the axisymmetric MWPotential2014 does not significantly affect heliocentric orbits within 100 AU and time integrations of 50 Eris years. Consequently, the trajectories are effectively indistinguishable.

$$a = 66.746\ AU \quad ; \quad e = 0.566 \quad ; \quad i = 0.665\ rad$$
$$\Omega = 0.559\ rad \quad ; \quad \omega = 3.524\ rad \quad ; \quad f = 1.002\ rad$$

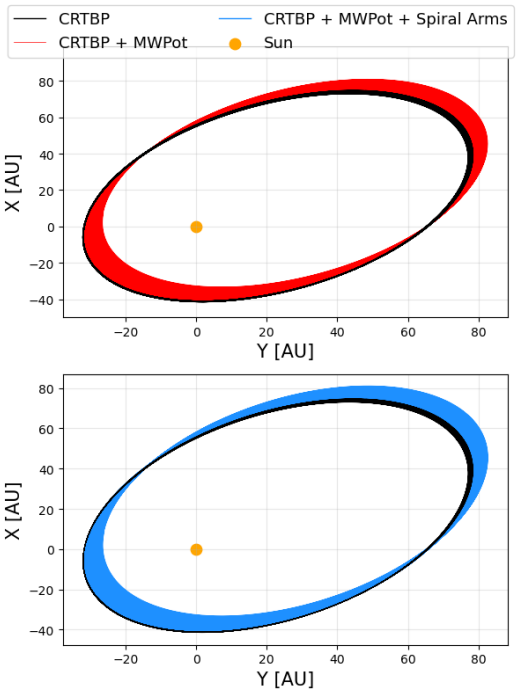

FIG. 4: Eris evolution with contributions of the CRTBP (black), MWPotential2014 (red) and Spiral Arms (blue).

V. RESULTS FOR A SUN-BOUND ASTEROID WITH A SEMI-MAJOR AXIS OF 530 AU

Using an example asteroid with a semi-major axis of 530 AU, the impact of the Milky Way potential is going

to be substantially stronger than before, as the force of the CRTBP will be reduced. This apparently arbitrary value of the semi-major axis was chosen as it is the point where the ratio between the CRTBP force and the Galactic Potential's forces falls under 10 orders of magnitude.

The integration time will be higher, $t_{\text{int}} = 10^9$ days in 2.000.000 time-steps. This is because, using Kepler's Third Law, the determined orbital period for the example asteroid is $T \propto a^{3/2} \sim 4.453 \times 10^5$ Earth days; therefore, the integration is approximately 225 orbital years.

Initial orbital elements proposed for example asteroid:

$$a = 530\ AU \quad ; \quad e = 0.120 \quad ; \quad i = 0.524\ rad$$
$$\Omega = 2.094\ rad \quad ; \quad \omega = 0.785\ rad \quad ; \quad f = 0.175\ rad$$

1^{st} Case (CRTBP): As shown in the 1^{st} Case of Eris, the CRTBP does not alter the orbit's behavior after integration. The integrated trajectory, illustrated in black in Figure 5, serves as a benchmark for comparison with subsequent cases.

2^{nd} Case (MWPotential2014): The effects of the MWPotential2014 are shown at the top panel of Figure 5. It is distinguishable that the orbit remains bound to the Sun, but the asteroid's trajectory exhibits signs of precession or drift. The post-integration results are consistent with those of Eris' **2^{nd} Case**, with the larger changes observed in the semi-major axis, eccentricity, and inclination.

$$a = 552.477\ AU \quad ; \quad e = 0.503 \quad ; \quad i = 0.228\ rad$$
$$\Omega = 1.124\ rad \quad ; \quad \omega = 2.631\ rad \quad ; \quad f = 2.378\ rad$$

3^{rd} Case (MWPotential2014 + Spiral Arms): In the case of farther heliocentric objects, when the Spiral Arms potential with pitch angle $\alpha = 9.5°$ is added to the axisymmetric MWPotential2014, it is observable that the contribution from the axisymmetric potential still dominates the orbital dynamics (see Figure 6). Opposed to the **3^{rd} Case** from Eris, the mean orbital elements do change, and we can see a more bound, less eccentric and inclined orbit.

$$a = 525.043\ AU \quad ; \quad e = 0.121 \quad ; \quad i = 0.545\ rad$$
$$\Omega = 0.657\ rad \quad ; \quad \omega = 2.284\ rad \quad ; \quad f = 3.187\ rad$$

Pitch angle comparison: The Spiral Arms are added to the MWPotential2014 as a perturbative component, due to their small contribution to the total Galactic potential. Here, we assess the influence of the pitch angle on the Galactic potential by studying the contribution of different spiral loci. The pitch angle α is varied within observational constraints for the Milky Way: with $\alpha = 9.5°$ the Solar System lies within a spiral arm, whereas for $\alpha = 15°$ it is located between two arms. In the middle, $\alpha = 11°$ corresponds to the default value adopted from Cox & Gómez (2002) [8].

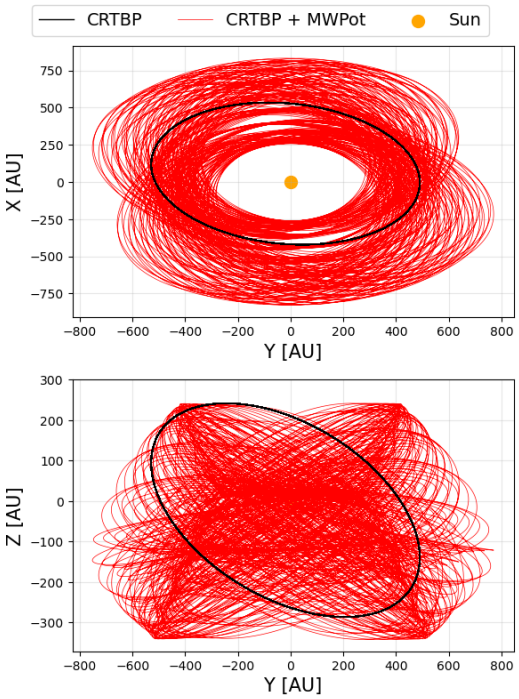

FIG. 5: Example's asteroid evolution for CRTBP with the axisymmetric MWPotential2014.

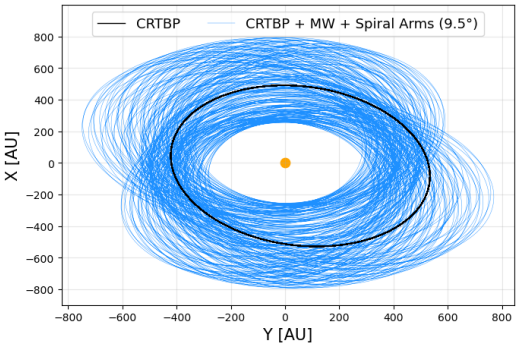

FIG. 6: Example's asteroid evolution with the MWPotential2014 + Spiral Arms potential.

As shown in Figure 7, the asteroid's orbital behavior is strongly dependent on the spiral-arm pitch angle. For $\alpha = 9.5°$, the orbit transitions to a more bound and nearly circular configuration, in contrast to the behavior when only using the axisymmetric MWPotential2014. Conversely, for $\alpha = 15°$, the orbit becomes wider and more eccentric, accompanied by a decrease in inclination.

To better asses the differences between pitch angle contributions, the distance at aphelion $d_{\text{aphelion}} = a(1+e)$ and the orbital elements from Table I will be analyzed.

$$d_{\alpha=9.5°} \simeq 589.10\,\text{AU} \quad d_{\alpha=11°} \simeq 636.22\,\text{AU}$$
$$d_{\alpha=15°} \simeq 718.45\,\text{AU} \quad d_{\text{Initial}} \simeq 593.60\,\text{AU}$$

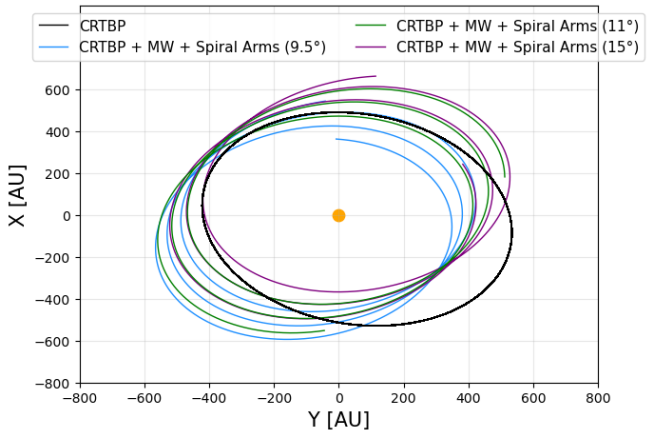

FIG. 7: Example's asteroid evolution with CRTBP + MWPotential2014 + Spiral Arms with different pitch angles $\alpha = 9.5°$(blue), $11°$(green) & $15°$(purple), all with amp=0.4. Only the last 25000 time-steps are shown for better visualization.

TABLE I: Example's asteroid evolution with different pitch angles, CRTBP + MWPotential2014 + Spiral Arms.

	Initial	MWPot	$\alpha = 9.5°$	$\alpha = 11°$	$\alpha = 15°$
a ±0.001 (AU)	530.000	552.477	525.043	511.023	539.378
e ±0.001	0.120	0.503	0.121	0.245	0.332
i ±0.001 (°deg)	30.000	13.077	31.330	26.193	24.922

These results indicate that a pitch angle of $\alpha = 9.5°$ effectively compensates the influence of the MWPotential2014, yielding an outcome that seems stable with a slow evolution over time. For $\alpha = 11°$ and $\alpha = 15°$, the Spiral Arms potential contributes to maintaining a more tightly bound orbit, although the MWPotential2014 continues to dominate the evolution of eccentricity and inclination. The full representation of all different pitch angle trajectories can be seen in Appendix D.

VI. CONCLUSIONS

In this project we have combined, for the first time, both gravitational potentials that may have an influence on the Solar System, namely the CRTBP and the Galactic potential. For the latter, we have considered both an axisymmetric only potential and the addition of a non-axisymmetric Spiral Arms potential. The conclusions obtained from this work are the following:

- The axisymmetric MWPotential2014 contributes to more eccentric and less inclined orbits, while also yielding higher semi-major axis values.
- The addition of the nonaxisymmetric Spiral Arms to the MWPotential2014 has no impact, beyond secular changes, at distances near 100 AU and integration times of 50 orbital years.
- The addition of the Spiral Arms to the MWPotential2014, near distances of 600 AU and integration times of about 225 orbiting years, has a significant effect on the trajectory of the minor body. The contribution is most notable in the reduction of the semi-major axis, eccentricity and inclination. Thus effectively compensating some of the effects of the MWPotential2014 over the minor body's trajectory and evolution. Such results indicate that adding a Spiral Arms could have an impact on the minor bodies of the Oort's Cloud.
- The pitch angle plays a key role in the non-axisymmetric Spiral Arms potential and its contribution to the Galactic potential.

Ultimately, we consider that the goal of this project is achieved. We have quantified, in terms of the mean orbital elements, the fact of including a Galactic potential on trajectories for minor bodies of the Solar System.

Acknowledgments

I would like to express my sincere gratitude to my advisor, Mercè Romero, for her constant support, insightful guidance, and for introducing me to this fascinating field. I am also thankful to my family and colleagues for their encouragement and support throughout this journey.

[1] Tanga, P., Pauwels, T., Mignard, F., Muinonen, K., Cellino, A., David, P., Hestroffer, D., Spoto, F., Berthier, J., Guiraud, J., et al., AA **674**, A12 (2023).
[2] J. Heisler and S. Tremaine, Icarus **65**, 13 (1986).
[3] J. Bovy, arXiv:1412.3451 [astro-ph.GA] (2014).
[4] J. E. Prussing and B. A. Conway, *Orbital Mechanics* (Oxford University Press, New York & Oxford, 1993).
[5] V. G. Szebehely, *The General and Restricted Problems of Three Bodies* (Springer, Vienna, 1974).
[6] G. Gómez, À. Jorba, J. J. Masdemont, and C. Simó, *Dynamics and Mission Design Near Libration Points, Vol. III: Advanced Methods for Collinear Points*, World Scientific Monograph Series in Mathematics (World Scientific, Singapore / River Edge, NJ, 2001).
[7] J. Bovy, The Astrophysical Journal Supplement Series **216**, 29 (2015).
[8] D. P. Cox and G. C. Gomez, The Astrophysical Journal Supplement Series **142**, 261–267 (2002).

Efectes del potencial Galàctic en objectes menors del Sistema Solar

Author: Pau Roca Acarin, procaaca27@alumnes.ub.edu
Facultat de Física, Universitat de Barcelona, Diagonal 645, 08028 Barcelona, Spain.

Advisor: Mercè Romero, mromero@fqa.ub.edu
(Dated: January 16, 2026)

Resum: Aquest projecte estudia la influència del potencial gravitatori Galàctic de la Via Làctia en l'evolució orbital d'objectes menors i llunyans del Sistema Solar. A partir de dades orbitals del Gaia Data Release 3, el moviment dels asteroides es modela mitjançant el Problema Circular Restringit de Tres Cossos (Sol–Júpiter–Objecte menor), incorporant les pertorbacions galàctiques com una força externa. Es consideren dos models galàctics: el potencial axisimètric MWPotential2014 i un no axisimètric de Braços Espirals implementat amb la llibreria `galpy`. Es fa ús d'integracions numèriques per analitzar les variacions seculars dels elements orbitals en escales temporals llargues. L'estudi es centra en el planeta nan Eris i en un asteroide hipotètic lligat al Sol amb un semieix major de 530 UA. Tot i que les forces Galàctiques són molt més febles que les del Sistema Solar, produeixen efectes mesurables a grans distàncies heliocèntriques: els efectes dels braços espirals són negligibles prop de 100 UA, mentre que ambdós components galàctics influeixen de manera significativa en l'estabilitat orbital més enllà de 500 UA, essent l'angle de pas dels braços espirals un factor clau.

Keywords: Potencial Galàctic, Dinàmica orbital d'objectes menors, Braços espirals, Pertorbacions seculars, Integració numèrica d'òrbites

ODSs: (4.) Educació de qualitat, (15.) Vida Terrestre i (9.) Indústria, Innovació, Infraestructures.

Objectius de Desenvolupament Sostenible (ODSs o SDGs)

1. Fi de la es desigualtats		10. Reducció de les desigualtats	
2. Fam zero		11. Ciutats i comunitats sostenibles	
3. Salut i benestar		12. Consum i producció responsables	
4. Educació de qualitat	X	13. Acció climàtica	
5. Igualtat de gènere		14. Vida submarina	
6. Aigua neta i sanejament		15. Vida terrestre	X
7. Energia neta i sostenible		16. Pau, justícia i institucions sòlides	
8. Treball digne i creixement econòmic		17. Aliança pels objectius	
9. Indústria, innovació, infraestructures	X		

Appendix A: Orbital Elements

The orbital elements are a set of coordinates that simplify the characterization of trajectories and orbits. These elements vary slowly in time and are well suited for analytical and secular orbit analysis; as such, having the orbital elements is equivalent as having a particular position in the orbit. In Chapter 3 of the Prussing and Conway '*Orbital Mechanics*' [4] there is a more detailed explanation and representation of the mean orbital elements.

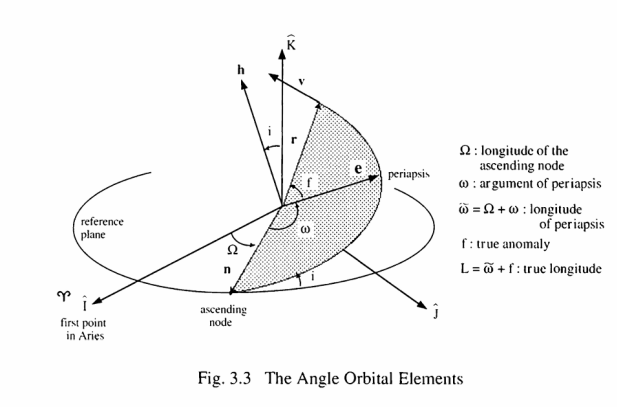

Fig. 3.3 The Angle Orbital Elements

FIG. 8: Image extracted from Chapter 3 of Prussing and Conway '*Orbital Mechanics*' [4].

Appendix B: Circular Restricted Three-Body Problem

The CRTBP hypotheses only consider the motion of a massive body orbiting an almost-static massive body and a third body with negligible mass orbiting both bodies, which are the Sun and Jupiter. To determine the equations of motion of the asteroid inside the Solar System, the Circular Restricted Three-Body (CRTBP) solution will be used.

The CRTBP equations do not include a z-axis solution for Jupiter; therefore, its orbit is confined to the XY-plane.

$$\begin{aligned} \dot{x} &= p_x + y \qquad \dot{y} = p_y - x \qquad \dot{z} = p_z \qquad \text{(B1)} \\ \dot{p_x} &= p_y - \frac{1-\mu}{r_{as}^3}\cdot(x-y) - \frac{\mu}{r_{aj}^3}\cdot(x-\mu-1) \\ \dot{p_y} &= -p_x - \Big(\frac{1-\mu}{r_{as}^3} + \frac{\mu}{r_{aj}^3}\Big)\cdot y \\ \dot{p_z} &= -\Big(\frac{1-\mu}{r_{as}^3} + \frac{\mu}{r_{aj}^3}\Big)\cdot z \end{aligned}$$

Where we have defined μ as the ratio between two masses, also the distances r_{as} and r_{aj} as:

$$\begin{aligned} r_{as}^2 &= (x-\mu)^2 + y^2 + z^2 \\ r_{aj}^2 &= (x-\mu+1)^2 + y^2 + z^2 \end{aligned}$$

For a more detailed explanation, see Szebehely [5].

Appendix C: Axisymmetric MWPotential2014

The Galactic potential, $\Phi_{\rm gal}$, represents the smooth and axisymmetric gravitational field of a given galaxy. Thus, the mathematical expression for the axisymmetric MW model, as given in section 3.5 of Bovy et al (2015) [7], is:

$$\Phi_{\rm gal}(\mathbf{r}) = \Phi_{\rm bulge}(\mathbf{r}) + \Phi_{\rm disk}(\mathbf{r}) + \Phi_{\rm halo}(\mathbf{r}),$$

where $\mathbf{r} = (x, y, z)$ denotes the Galactocentric position vector. The analytical forms of the equations:

$$\begin{aligned} \Phi_{\rm bulge}(r) &= \text{amp}\Big(\frac{r_1}{r}\Big)^{\alpha}\cdot e^{-(r/r_c)^2} \\ \Phi_{\rm disk}(R,z) &= -\frac{\text{amp}}{\sqrt{R^2 + \big(a + \sqrt{z^2+b^2}\big)^2}} \qquad \text{(C1)} \\ \Phi_{\rm halo}(r) &= -\frac{\text{amp}}{4\pi\, a^3}\frac{1}{(r/a)\cdot(1+r/a)^2} \end{aligned}$$

The value of all non-determined variables, along with a more in depth explanation, can be found in Bovy et al (2015) [7].

Appendix D: Trajectory computation: CRTBP + MWPotential2014 + Spiral Arms

As seen in Table I, the pitch angle plays a key role to the contribution of the Spiral Arms in the Galactic Potential. As such, the trajectory is largely influenced and, over time, the effects become more and more apparent.

For a better visualization of the evolutions described by all three cases of the pitch angle (α), this appendix serves as a visual aid to further comprehend the results obtained in Figure 7.

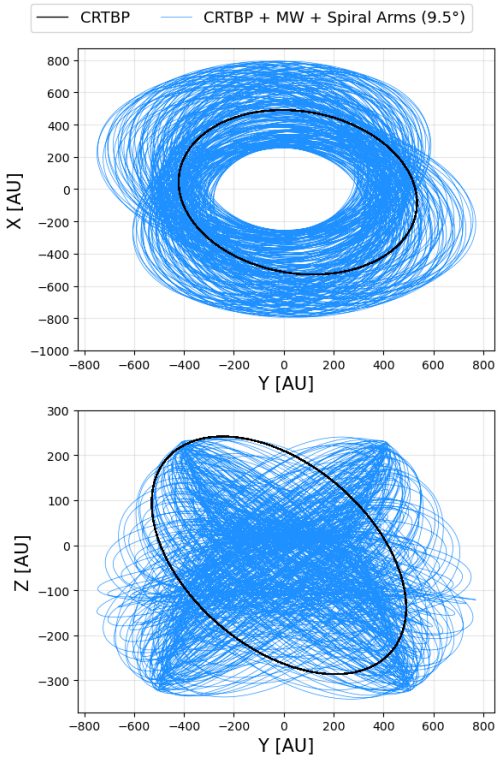

FIG. 9: Example asteroid orbit's evolution with CRTBP + MWPotential2014 + Spiral Arms ($\alpha = 9.5°$).

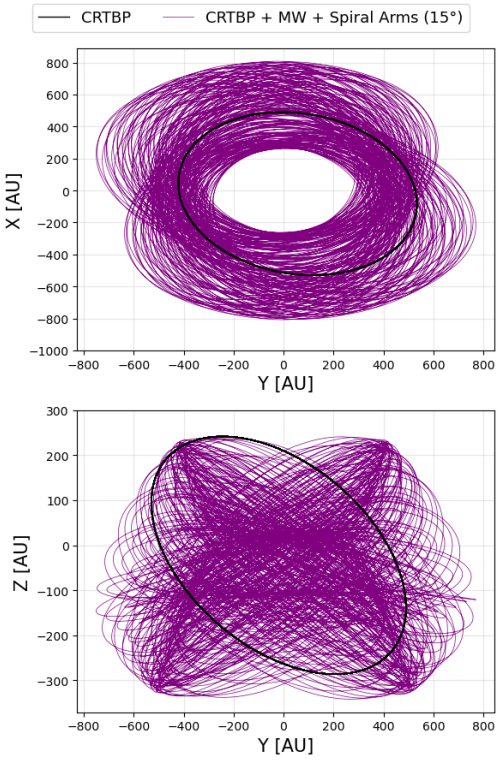

FIG. 11: Example asteroid orbit's evolution with CRTBP + MWPotential2014 + Spiral Arms ($\alpha = 15°$).

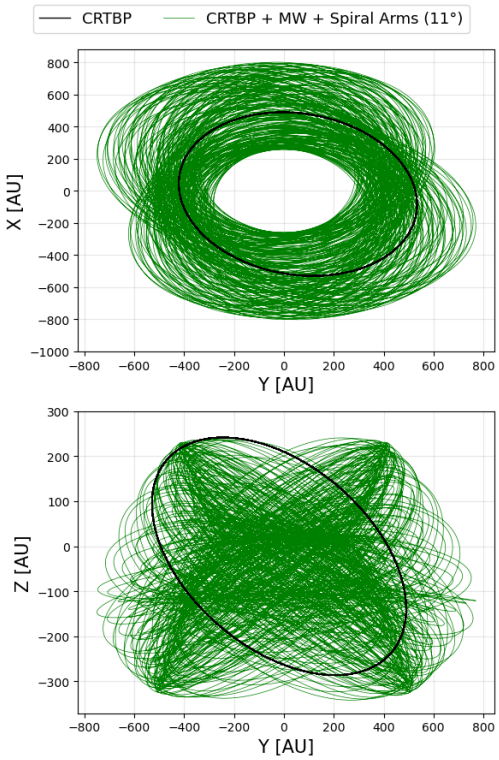

FIG. 10: Example asteroid orbit's evolution with CRTBP + MWPotential2014 + Spiral Arms ($\alpha = 11°$).